

IFSCC 2025 full paper (IFSCC2025-1190)

Enhancing Sun Protection Factor of O/W Sunscreen by Modifying Droplet Shape through Regulating Interfacial Crystallization of Oil-Phase Component

Chuancheng Wang¹, Yuhang Liu¹, Jihua Wei^{* 2}, Yuyan Chen¹, Jie Zhou¹, Hong Yu Dong¹, Meng Tang¹, Peiwen Sun¹

¹Research & Innovation Center, ²International Academy of science, Proya Cosmetics Co., Ltd. , Hangzhou, China

1. Introduction

In recent years, due to environmental pollution, which has destroyed the ozone layer, ultraviolet (UV) intensity has increased, leading to a series of skin problems such as increased skin sensitivity, accelerated melanin synthesis, and skin cancer induction [1,2]. Consequently, consumers have become more aware of sun protection, driving the growth of the sunscreen market [3-8]. While sunscreen with a high sun protection factor (SPF) is widely acknowledged to offer superior UV protection, this often requires the addition of more UV filters. However, these UV filters have been proven to potentially impact coral reef bleaching, the food chain, and human health [9-12]. Therefore, there is an urgent need to develop effective strategies to enhance the UV-shielding efficiency of sunscreens without relying on high levels of UV filters.

Interestingly, particles that exhibit light-scattering properties can significantly enhance sunscreen's UV protection [13-17]. For example, Lademann et al. proved that particles with light-scattering properties can increase the optical pathway of photons in an absorbing medium, thereby enhancing photon absorption in the medium. They used Monte Carlo calculations and Evans blue pigment tests to demonstrate this effect [15]. Herzog et al. also found that different particle sizes of a benzotriazole derivative exhibit different UV protection properties. They used ball milling to micronize the particles and discovered that when the particle size was 80 nm, the benzotriazole derivative showed the best UV-shielding efficiency. Reflecting spectroscopic measurements indicated that scattering contributes to 10% of the UV-attenuating effect, comprising 7% forward scattering and 3% back scattering, while absorption accounted for 90% [17]. Nowadays, spherical polymer particles, such as styrene/acrylates copolymer, are widely recommended to be added to sunscreens at concentrations of 3%–5% to enhance UV protection efficiency. However, while studies of light-scattering particles typically focus on spherical particles, the effects of particles' morphology on UV performance boosting have been studied less. In optics, it has been proven that irregularly shaped particles have different light-scattering properties compared to spherical particles. Fan et al.'s work showed that at certain back-scattering angles (120°–180°), the scattering efficiency was much higher than that of spherical particles. This indicated that using irregularly shaped particles in sunscreens may result in

better UV performance boosting compared to spherical particles [18]. However, incorporating 3%–5% particles poses a challenge to the skin feel and cost of sunscreens.

In Liu et al.'s study, lipid crystallization inside oil droplets modified the properties of oil-in-water (O/W) emulsions. The specific wax induced the formation of new hydrocarbon chain distances and decreased the lamellar distance of the single crystallites. As a result, large and rigid crystals formed within the droplets, transforming the spherical droplets into irregularly shaped droplets [19]. Herein, we screened the oil crystallization component and creatively found a specific proportion of fatty alcohol, glycoside emulsifiers, and poly C10-30 alkyl acrylate as an irregularly-shaped form composition that could produce an O/W sunscreen with irregularly shaped droplets. We tested the degree of irregularity, microstructure after spreading, and the performance of UV protection boosting in different formulations. In addition, a combination of testing and characterization was used to analyze the mechanisms of the formation of the sunscreen with irregularly shaped droplets and its role in enhancing UV protection.

2. Materials and Methods

2.1. Materials

All reagents were purchased from raw material vendors and used directly without further purification. The ingredients used in the experiment are listed according to the International Nomenclature of Cosmetic Ingredients: deionized water; carbomer; acrylates/C10-30 alkyl acrylate crosspolymer; propanediol; phenoxyethanol; ethylhexylglycerin; bis-ethylhexyloxyphenol methoxyphenyl triazine; ethylhexyl triazone; diethylamino hydroxybenzoyl hexyl benzoate; ethylhexyl methoxycinnamate; isononyl isononanoate; C14-22 alcohols; C12-20 alkyl glucoside; cetearyl alcohol; cetearyl glucoside; poly C10-30 alkyl acrylate; vinyl pyrrolidone/eicosane copolymer; triacontanyl Polyvinyl pyrrolidone(PVP); potassium cetyl phosphate; CI 42090; carotene; methylene bis-benzotriazolyl tetramethylbutylphenol; decyl glucoside; propylene glycol; parfum.

2.2. Preparation of Sunscreen Samples

The sunscreen with irregularly shaped droplets were created using a composition consisting of three components: C14-22 alcohols, C12-20 alkyl glucoside, and poly C10-30 alkyl acrylate. These components share similar alkyl chain structures.

The formulation of the sunscreen sample containing the composition is presented in Table 1. The procedure was carried out as described below: Initially, phase A and phase B were heated to 78–80 °C and homogenized through a blender individual. Subsequently, phase B was gradually added to phase A while stirring continuously to ensure uniform mixing, followed by emulsification with a homogenizer at a speed of 8000 rpm for 5 minutes. After that the lotion was cooled to the room temperature. This resulted in the formation of the sunscreen with irregularly shaped droplets designated as IS.

Control samples preparation: Based on the method and formulation described above, poly C10-30 alkyl acrylate was removed to create a blank control sample, labeled as BL. In another sample, Additionally, the fatty alcohols and glucoside emulsifier were replaced with cetearyl alcohol and cetearyl glucoside to obtain another control sample, labeled as CA. Finally, poly C10-30 alkyl acrylate was replaced with triacontanyl PVP to create control sample with another film-forming polymer, labeled as TP.

2.3. Micromorphological Characterization of sunscreen sample's droplet

The microstructures of the samples were assessed using an optical microscope. The sunscreen samples were dripped onto a slide and covered with a coverslip to investigate the microstructures and to determine the proportion of irregularly shaped droplets. The proportion of irregularly shaped droplets in the sunscreen samples was used to define as the irregularity degree of the sample, for example, if the proportion was greater than or equal to 80% but less than 81%, the irregularity degree was defined as 80%.

Table 1. The formulation of the sunscreen sample containing the composition (IS)

| Phase | Component | Content(%) |
|-------|--|------------|
| A | Deionized water | To 100 |
| | Carbomer | 0.5 |
| | Acrylates/C10-30 Alkyl Acrylate Crosspolymer | 0.2 |
| | Propanediol | 5 |
| | Phenoxyethanol | 1 |
| | Ethylhexylglycerin | 1 |
| | Potassium Cetyl Phosphate | 0.2 |
| B | Bis-ethylhexyloxyphenol | 2.5 |
| | Methoxyphenyl Triazine | |
| | Ethylhexyl Triazole | 1 |
| | Diethylamino Hydroxybenzoyl Hexyl Benzoate | 2 |
| | Ethylhexyl Methoxycinnamate | 4 |
| | Isononyl Isononanoate | 4 |
| | C14-22 alcohols | 0.96 |
| | C12-20 alkyl glucoside | 0.24 |
| | Poly C10-30 alkyl acrylate | 0.4 |

2.4. Differential scanning calorimetry (DSC) measurements

The thermal profiles of the compositions were analyzed using DSC. The C14-22 alcohols and C12-20 alkyl glucoside were mixed to form sample A at a mass ratio of 4:1. C14-22 alcohols, C12-20 alkyl glucoside, and poly C10-30 alkyl acrylate were mixed to form sample B at a mass ratio of 3.5:1:1.7. Cetearyl alcohol, cetearyl glucoside and poly C10-30 alkyl acrylate were mixed to form sample C at a mass ratio of 3.5:1:1.7. C14-22 alcohols, C12-20 alkyl glucoside and triacontanyl PVP were mixed to form sample D at a mass ratio of 3.5:1:1.7.

During the test, the samples were kept at 10°C for 5 minutes, then heated at a rate of 5°C/min to 85°C, kept at 85°C for 5 minutes, and finally cooled at a rate of 5°C/min back to 10°C. The temperatures of the peaks and the enthalpies of melting were calculated using the DSC NETZSCH Proteus software. All analyses were performed in triplicate.

2.5. In Vitro Sun Protection Value Test

The procedure for in vitro sun protection value test adhered to the ISO 24443:2021 standard [20]. Sunscreen samples IS, BL, CA and TP were individually applied to a HD6-type PMMA plate (measuring 5 cm by 5 cm) at a loading rate of 1.3 mg/cm²[20]. Each sample was dispensed as at least twelve small droplets of approximately equal volume, which were evenly distributed across the entire surface of the plate. Subsequently, the samples were spread uniformly to cover the entire area of the plate. After that, the PMMA plates were dried at room temperature in a dark environment for 30 minutes. The SPF and the UVA Protection Factor

(PFA) were determined using a UV transmittance analyzer. For each sunscreen sample, four PMMA plates were prepared, and the average value obtained from these measurements was recorded as the initial overall protection value of the sample.

2.6. Staining test

To investigate the differences in the microstructures of the oil phase after spreading sunscreens with irregularly shaped droplets and spherical droplets, samples IS and TP were dyed using a staining method and observed under an optical microscope after spreading on slide. The sunscreen samples were stained with blue water-soluble pigment(CI 42090) and carotene, then applied onto a slide at a loading of 2 mg/cm² and an application area of 2 cm × 2 cm. The microstructures of the sunscreen were photographed after 5 minutes and 2 hours.

2.7. In vivo Sun protection value test

To learn more about the effect of irregularly shaped droplets on sun protection value in commercial sunscreen, we prepared two commercial sunscreen samples with or without irregularly shaped droplets, and an in vivo sun-protection value test was conducted. The test was performed using a human efficacy experimental assessment method adhered to the ISO 24444:2019 standard [21]. A UV solar simulator was used. During the test, the standard techniques outlined in the Safety and Technical Specifications for Cosmetics (2022) were followed, the ethical standards of the Declaration of Helsinki (1975, revised in 2013) were adhered to, and all participants signed an Informed Consent Form. The commercial sunscreens' formulation were shown in Table 2.

Table 2. The formulation of the commercial sunscreen samples

| Phase | Component | Sample A | Sample B |
|-------|---|----------|----------|
| A | Deionized water | To 100 | To 100 |
| | Carbomer | 0.5 | 0.5 |
| | Acrylates/C10-30 Alkyl Acrylate Crosspolymer | 0.2 | 0.2 |
| | Propanediol | 5 | 5 |
| | Phenoxyethanol | 1 | 1 |
| | Ethylhexylglycerin | 1 | 1 |
| B | Potassium Cetyl Phosphate | 0.2 | 0.2 |
| | Bis-ethylhexyloxyphenol | 2.5 | 2.5 |
| | Methoxyphenyl Triazine | | |
| | Ethylhexyl Triazone | 1 | 1 |
| | Diethylamino Hydroxybenzoyl Hexyl Benzoate | 2 | 2 |
| | Ethylhexyl Methoxycinnamate | 4 | 4 |
| | Isononyl isononanoate | 4 | 4 |
| | C14-22 alcohols | 0.96 | 0.96 |
| | C12-20 alkyl glucoside | 0.24 | 0.24 |
| | Poly C10-30 alkyl acrylate | 0.4 | / |
| C | Methylene Bis-Benzotriazolyl Tetramethylbutylphenol | 3 | 3 |
| | Decyl Glucoside | 0.45 | 0.45 |
| | Propylene Glycol | 0.024 | 0.024 |
| | Deionized water | 2.5 | 2.5 |
| D | Parfum | 0.5 | 0.5 |

3. Results

3.1. Micromorphological Analysis of the sunscreen samples

Firstly, the microscopic structures of the prepared sunscreen samples were observed using an optical microscope to verify the impact of different crystallizable oil-phase components on the morphology of the droplets within the sunscreen samples. Figure 1 shows the morphology of all samples as observed under the optical microscope. It is evident that samples IS and CA have distinctly irregularly shaped droplets, while the remaining samples exhibit spherical droplets.

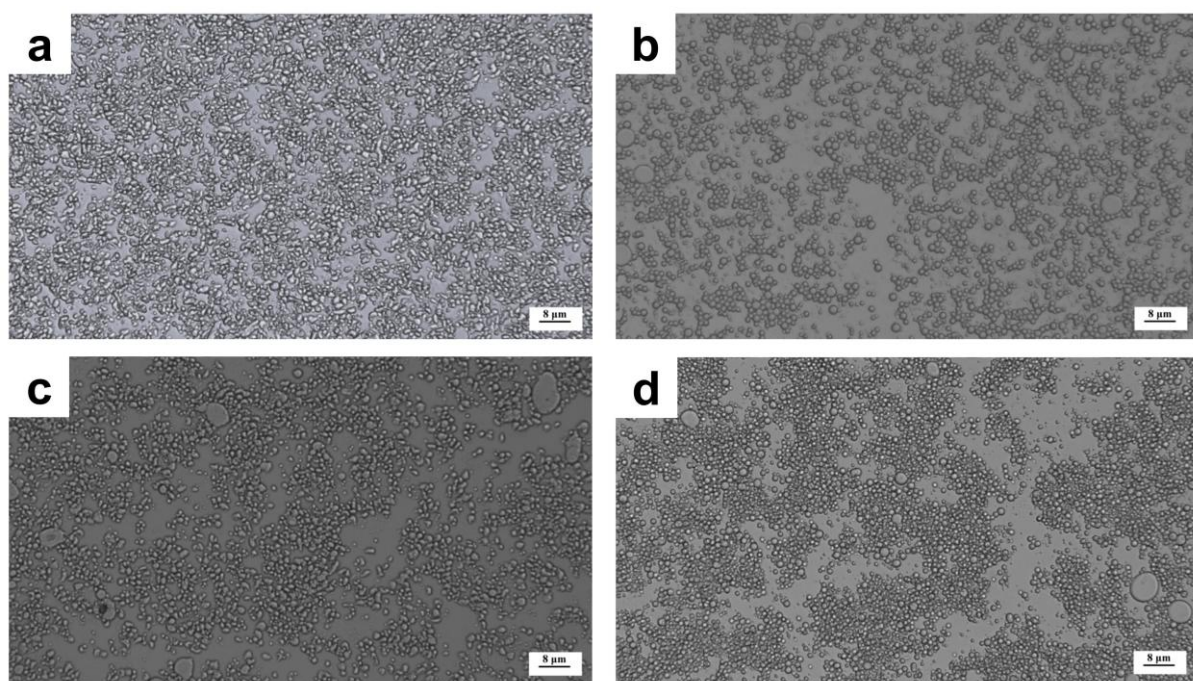


Figure 1. Microstructures of the droplet of sunscreen samples (a) IS, (b) BL, (c) CA, (d) TP.

3.2. Irregularity degree of the sunscreen samples

To further explore the irregularity degree of the samples, the proportion of irregularly shaped droplets within the samples was determined. The proportion of irregularly shaped droplets in samples IS and CA exceeded 85%, as shown in Table 3. In contrast, the proportion in the remaining samples was lower than 10%.

Table 3. Irregularity degree of all sunscreen samples.

| Sample | Irregularity degree |
|--------|---------------------|
| IS | 90% |
| BL | 85% |
| CA | 10% |
| TP | 8% |

3.3. DSC tests of the sunscreen samples

To further investigate the mechanism of irregularly shaped droplet formation, we conducted DSC tests on the different kinds of oil-crystallizable composition and observed the characteristic peaks during the cooling and melting processes of the tested samples. The test results are shown in Figure 2. During the cooling process, Sample A exhibited three distinct crystallization peaks, located at 24.9°C, 54.1°C, and 62.2°C, respectively. In contrast, after the addition of poly C10-30 alkyl acrylate (Sample B), the crystallization peak at 24.9°C disappeared, and a new crystallization peak emerged at 37.0°C. Sample C, which replaced the C14-22 alcohols and C12-20 alkyl glucoside in Sample B with cetearyl alcohol and cetearyl glucoside, also displayed a similar distribution of crystallization peaks at 37.8°C. Sample D, which replaced the poly C10-30 alkyl acrylate in Sample B with triacontanyl PVP, showed only a broad crystallization peak during the cooling process. These results suggest that poly C10-30 alkyl acrylate interacts with the alkyl chains of glycoside emulsifiers and long-chain fatty alcohols, thereby increasing the crystallization temperature of low-melting-point substances. Meanwhile, triacontanyl PVP also results in similar interactions; however, the absence of distinct peaks indicates that the combination of triacontanyl PVP, fatty alcohols, and glycoside emulsifiers has a slower crystallization rate[22].

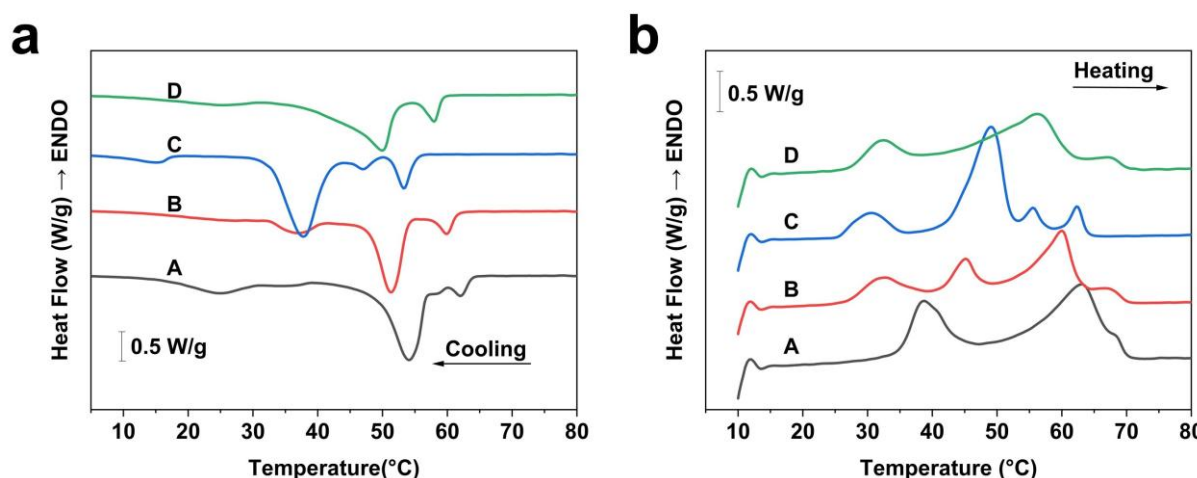


Figure 2. DSC thermographs of sample A, B, C, and D during the cooling (a) cycle at 5 °C/min and the heating (b) cycle at 5 °C/min. Insets: zoom in on the y-axis.

3.4. *In vitro* Sun protection value test

After that, we tested the *In vitro* Sun Protection Value properties of the samples. The *In vitro* SPF test results are shown in Table 3. The results showed that the samples with irregularly shaped droplets, namely IS and CA, exhibited higher *In vitro* SPF and PFA values (IS: SPF 58, PFA 10.2; CA: SPF 58, PFA 10.4), whereas the samples with spherical droplets, BL and TP, had lower *In vitro* SPF and PFA values (BL: SPF 21, PFA 6.8; TP: SPF 29, PFA 7.3). This is also similar to our predicted results, indicating that irregularly shaped droplets have the effect of enhancing the sun protection value of sunscreen.

Table 3. *In vitro* Sun Protection Value results of sunscreen samples

| Sample | SPF(<i>In-vitro</i>) | PFA(<i>In-vitro</i>) |
|--------|------------------------|------------------------|
| IS | 58 | 10.2 |
| BL | 21 | 6.8 |
| CA | 58 | 10.4 |
| TP | 29 | 7.3 |

3.4. Staining test

Subsequently, we conducted staining test to observe the microstructures of sunscreen samples IS and TP after spreading on a slide. Carotene was used as the oil-phase pigment, while a blue water-soluble pigment (CI 42090) was employed for the water phase. Optical microscopy was performed at 5 minutes and 2 hours post-spreading. The results are shown in Figure 3. The images reveal that the microstructures of IS was significantly different from TP at both 5 minutes and 2 hours post-spreading. At 5 minutes, the droplet shapes of the IS were notably more irregular. After 2 hours, the film area of the IR samples was larger, with some regions still containing irregularly shaped particles (circled in red). In contrast, no such irregularly shaped particles were observed in the TP samples. These differences in surface morphology after spreading may account for the higher SPF and PFA values observed for the irregularly shaped IS samples in the in vitro sun protection value tests.

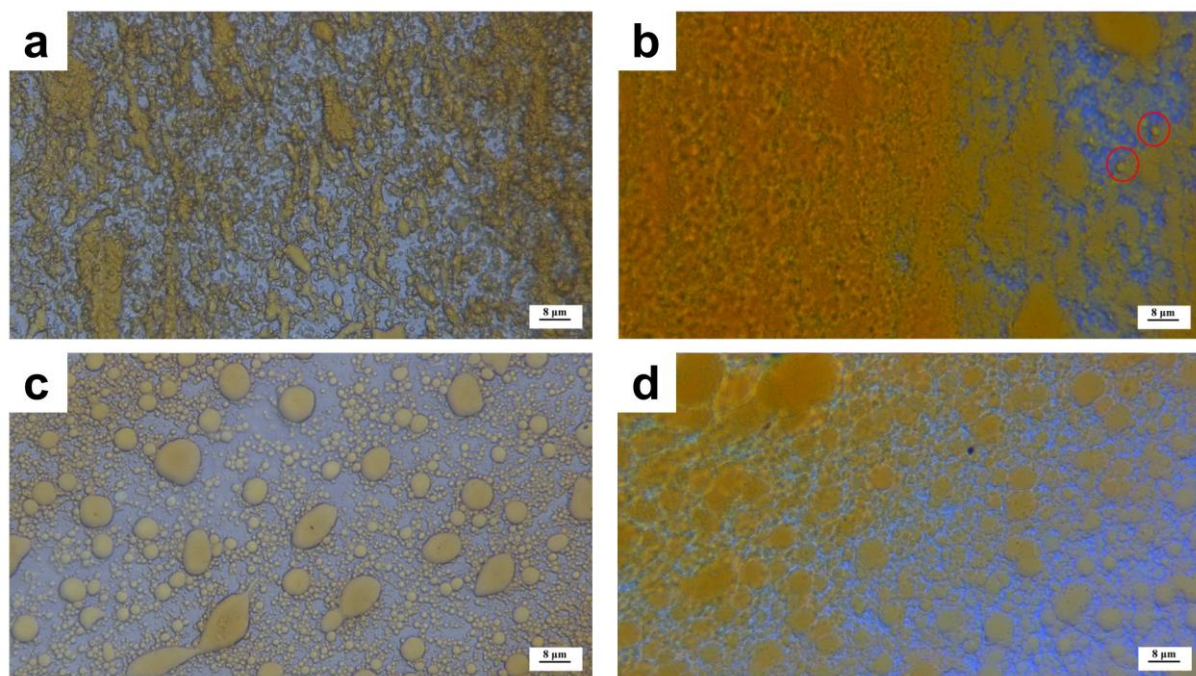


Figure 3. Microscopic evaluation of an sunscreen samples containing carotene and a blue water-dispersed pigment (a) IS photographed after spreading 5 minutes; (b) IS photographed after spreading 2 hours; (c) TP photographed after spreading 5 minutes; (d) TP photographed after spreading 2 hours.

3.5. In vivo Sun protection value test

In order to further verify the effect of irregularly shaped droplet on the sun protection index of sunscreen and the application of this finding in commercial products, we tested the sunscreens A and B by in vivo sun protection value test. Ten eligible participants were recruited for the test. The test results are shown in Table 5. Sunscreen with irregularly shaped droplets exhibited higher SPF values in in vivo sun protection value tests. Specifically, Sample A with irregularly shaped droplets SPF was 75, while sphericial droplets Sample B was 56.

Table 5. The in-vivo Sun Protection Value results of commercial sunscreen samples

| Commercial sunscreen sample | SPF(In-vivo) |
|------------------------------------|---------------------|
| A | 75 |
| B | 56 |

4. Discussion

The addition of 3%–5% of spherical particles with light-scattering properties to sunscreen has been recognized as an effective method to enhance the SPF and PFA values [13-17]. However, the impact of particle morphology on the enhancement of sun protection efficacy remains underexplored. Compared to spherical particles, irregularly shaped particles are believed to exhibit different light-scattering capabilities in terms of optical properties [18]. Therefore, we aim to incorporate irregularly shaped particles into sunscreen and investigate the impact of particle morphology on sun protection efficacy.

However, the introduction of high concentrations of inorganic particles poses challenges in terms of both product texture and cost. In O/W emulsions, certain crystallizable natural waxes have been demonstrated to alter the morphology of emulsions during the crystallization process [19]. Therefore, we attempted to introduce oil-phase crystallizable substances into O/W sunscreen to modify the morphology of the droplets of the sunscreen. Glycoside emulsifiers have been shown to form liquid crystal emulsions when combined with fatty alcohols, while some film-forming polymers are also believed to possess crystallization capabilities. Therefore, we focused on crystallizable emulsifiers and film-forming polymers to investigate the formation of irregularly shaped droplets in sunscreen.

Upon observation using optical microscopy, it was found that the IR and CA, which were formulated with fatty alcohols, glycoside emulsifiers, and poly(C10-30) alkyl acrylate copolymers, exhibited pronounced irregularly shaped droplets. Conversely, no such effect was observed when the formulation replaced poly(C10-30) alkyl acrylate copolymers with triacontanyl PVP film-forming polymer (TP) or removed the copolymers (BL).

To further explore the mechanisms, we conducted DSC on the composition of fatty alcohols, glycoside emulsifiers and film-form agents. The results indicated that poly(C10-30) alkyl acrylate copolymers exhibit significant alkyl chain interactions with long-chain fatty alcohols and glycoside emulsifiers. When these components are combined, the crystallization peak during cooling, which is typically observed at 24.9°C, shifts to higher temperatures, 37°C. This shift suggests that the crystalline structures formed by this combination may persist on the skin when the sunscreen is applied, thereby providing a scattering effect. In contrast, the DSC thermogram of triacontanyl PVP displays a broad single peak with a long melting range. This indicates that the crystallization rate is slower when triacontanyl PVP is incorporated. The slower crystallization rate may hinder the formation of crystalline structures in practical formulations, and consequently, prevent the development of sunscreen with irregularly shaped droplets[22].

Subsequently, we evaluated the in vitro sun protection values of the samples. The results demonstrated that emulsions with irregularly shaped droplets exhibited higher in vitro SPF values compared to those without such irregular morphology. Specifically, after incorporating poly(C10-30) alkyl acrylate copolymers, the SPF of sample IS increased by 176% relative to sample BL, while the SPF of sample TP increased by only 38%.

To further investigate the differences in morphology after spreading between sunscreen with irregularly shaped droplets and those with spherical droplets after application, we conducted application experiments on samples IS and TP following staining. The application results revealed that, even after 2 hours, sample IS still exhibited a few irregular particles. This observation suggests that the crystalline structures formed by the crystallizable components in the oil phase may persist after application. Consequently, these structures can enhance the light-scattering effect, thereby contributing to the improved sun protection value observed in the in vitro tests.

Finally, to verify the practical application of irregularly shaped emulsions in commercial sunscreen formulations, we prepared two commercial sunscreens: one with irregularly shaped emulsions and one without. We then conducted in vivo SPF tests on these products. The results indicated that the sunscreen with irregularly shaped emulsions exhibited a higher in vivo SPF value(75). These findings demonstrate that modifying the morphology of emulsion droplets in sunscreen by incorporating crystallizable oil-phase components can enhance the SPF values and is an effective strategy for improving sun protection efficacy in commercial formulations. The above results verified the effects of irregularly shaped droplets on sunscreen efficacy and proposed a novel approach to enhancing sun protection, thereby demonstrating the impact of droplet morphology on sunscreen performance.

5. Conclusion

The present study proposes a method to enhance the sun protection factor (SPF) of sunscreens by altering the morphology of the internal oil phase, and it demonstrates that irregularly shaped droplets exhibit superior light-scattering properties compared to spherical droplets. By incorporating oil-phase crystallizable components with similar alkyl chain structures into oil-in-water sunscreen emulsions, irregularly shaped droplets were introduced, thereby increasing the sun protection efficacy of the products. The improvement in performance is likely attributed to the enhanced light-scattering capability of irregular droplets, which increases the photon path length within the sunscreen film and subsequently improves the utilization efficiency of the UV filters. Specifically, the interaction between poly(C10-30) alkyl acrylate copolymers, fatty alcohols, and the alkyl chains of glycoside emulsifiers raises the crystallization temperature. This interaction enables the droplets within the emulsion to maintain a certain irregular morphology when applied, thus achieving better sun protection effects. In vitro testing revealed a 176% increase in the SPF value of sunscreens with irregular droplets, while in vivo testing showed a 33% enhancement in SPF value. In summary, this research will expand the application of irregularly shaped particles in sunscreens and provide new strategic insights for the development of sun protection products.

6. Reference

1. Yang et al.(2023) Ball-milling of titanium dioxide and zinc oxide for enhanced UV protection. *Frontiers in Materials* 10: 1273659.
2. Chen et al.(2024) Structural Similarity-Induced Inter-Component Interaction in Silicone Polymer-Based Composite Sunscreen Film for Enhanced UV Protection. *Polymers* 16: 3317.
3. Lee et al.(2020) Preparation and application of light-colored lignin nanoparticles for broad-spectrum sunscreens. *Polymers*, 12: 699.

4. Wang et al.(2018) Skin pigmentation-inspired polydopamine sunscreens. Advanced Functional Materials 28: 1802127.
5. Girard et al.(2024) The Impact of Lignin Biopolymer Sources, Isolation, and Size Reduction from the Macro-to Nanoscale on the Performances of Next-Generation Sunscreen. Polymers 16: 1901.
6. Cardillo, D., et al.(2021) Attenuation of UV absorption by poly (lactic acid)-iron oxide nano-composite particles and their potential application in sunscreens. Chemical Engineering Journal 405: 126843.
7. Lee, S.J., et al.(2024) Hyaluronic acid/polyphenol sunscreens with broad-spectrum UV protection properties from tannic acid and quercetin. International Journal of Biological Macromolecules 257: 128585.
8. Zhang, Z., et al.(2023) Mussel-inspired anti-permeation hybrid sunscreen with reinforced UV-blocking and safety performance. Colloids and Surfaces A: Physicochemical and Engineering Aspects 676: 132140.
9. van Bodegraven, M., et al.(2024) Redefine photoprotection: Sun protection beyond sunburn. Experimental Dermatology 33: e15002.
10. Hayag, M.V., et al.(1997) A high SPF sunscreen's effects on UVB-induced immunosuppression of DNCB contact hypersensitivity. Journal of Dermatological Science 16: 31–37.
11. Williams, J.D., et al.(2018) SPF 100+ sunscreen is more protective against sunburn than SPF 50+ in actual use: Results of a randomized, double-blind, split-face, natural sunlight exposure clinical trial. Journal of the American Academy of Dermatology 78: 902–910.
12. Shetty, N.,(2023) The effects of UV filters on health and the environment. Photochemical & Photobiological Sciences 22: 2463–2471.
13. Jones, C.,(2002) Hollow sphere technology for sunscreen formulation. SOFW Journal 128(9):36–40.
14. Herzog, B.,(2011) Influence of particles on the performance of sunscreens. 11th international sun protection conference. Summit Events, London.
15. Lademann, J., et al.(2005) Synergy effects between organic and inorganic UV filters in sunscreens. J Biomed Opt 10(1):14008.
16. Herzog, B., (2002) Prediction of sun protection factors by calculation of transmissions with a calibrated step film model. Journal of Cosmetic Science 53(1):11–26.
17. Herzog, B., et al.(2004) Physical properties of organic particulate UV absorbers used in sunscreens – II. UV-attenuating efficiency as function of particle size. Journal of Colloid and Interface Science 276(2):354–363.
18. Meng, F., et al.(2012) Scattering properties of non-spherical particles in the CO₂ shortwave infrared band. Acta Physica Sinica 61(20): 204202.
19. Liu, C.H., et al.(2021) Exploration of the natural waxes-tuned crystallization behavior, droplet shape and rheology properties of O/W emulsions. Journal of Colloid and Interface Science 587: 417-428.
20. ISO 24443:2021; Cosmetics—Determination of sunscreen UVA photoprotection in vitro. ISO: Geneva, Switzerland, 2021.
21. ISO 24444:2019; Cosmetics—In vivo determination of the sun protection factor (SPF). ISO: Geneva, Switzerland, 2019.
22. Freitas, G.B., et al.(2018) Influence of wax chemical structure on W/O emulsion rheology and stability. Colloids and Surfaces A: Physicochemical and Engineering Aspects 558: 45-56.